On-line process diagnosis of laser drilling in a liquid environment

I. NICOLAE[a], C. VIESPE[a,*], C. GHEORGHE[b], D. MIU[a]
[a]National Institute for Laser, Plasma and Radiation Physics, Laser Department, Atomistilor 409, 077125 Bucharest-Magurele, Romania
[b]JNO Group SRL, Str. Odai nr. 31, Jilava, Romania

Laser drilling of industrial steel and aluminum in a liquid environment was recorded using a 210× microscope at 40 frames/s. Computing the light emission intensity from recorded images revealed highly specific time evolution depending on the target material and laser repetition rate. A correlation between drilling depth and light emission intensity was made. Based on this correlation and specificity, real time drilling process monitoring and diagnosis should be possible. Mitigation of the effects of gas bubbles on laser-target interaction by heat treatment of the target in vacuum is also outlined.

1. Introduction

Laser ablation in liquids has already proven to be a remarkable tool for machining and material synthesis [1-8]. The confinement of ablated species in a liquid environment changes effects radically. Spatial confinement leads to development of extremely high pressures and temperatures, of the order of 10^9 Pa and 10^3 K, respectively [9]. Such energetic conditions make this method especially attractive for material removal, due to more efficient use of the laser energy [5]. This is explained by the fact that confined plasma acts as a highly effective cutting torch [10]. An additional material removal mechanism is caused by collapsing cavitation bubbles [11]. In total, there are three material removal mechanisms involved in laser ablation in liquids [6]: (1) direct laser ablation, (2) plasma corrosion, and (3) mechanical erosion by cavitation bubble collapse [10].

Visual analysis and investigation of laser ablation in a liquid environment were performed [12-14]. Laser ablation dynamics, shock wave propagation and cavitation bubble formation/collapse, all important effects of laser-matter interactions in a liquid environment, were studied. The purpose of the present work was to diagnose and quantify the evolution of processes occurring during laser drilling in a liquid environment on a nanosecond time-scale, with an emphasis on the possible use of digital imagery for real-time monitoring of the laser drilling depth. This was achieved by studying the light emission intensity variation due to drilling, for a 50 second laser irradiation time interval, and by relating it to drilling depth vs. irradiation time.

We consider that this method has potential for real-time, on-line laser process supervision and diagnostics. In order to monitor the drilling depth in real time by means of the emission intensity, the evolution of the light emission intensity must be monotonous; in these conditions, a one-on-one relationship between drilling depth and intensity emission can be made.

2. Experimental

A Nd:YVO$_4$ laser (Lumera Rapid) with an 8 ps pulse duration was used for the experiments. All the experiments were made using a wavelength of 1064 nm. The laser beam was focused onto the target surface using a 30 mm lens; the position of the focal point was constant during the entire drilling process.

Aluminum and industrial grade steel were used as target material, as in prior laser ablation in liquid experiments [15], allowing us to elaborate and clarify previous results. The target was placed vertically in a flux of tap water, inside a closed cell of 2 cm×4 cm×4 cm, placed on a manual micrometric xy table; the lens was mounted on a separate linear micrometric table. The water flowed with 3.3 l/minute in a direction parallel to the target surface, and perpendicular to the 2 cm × 4 cm cell section. This is equivalent with a water speed of ~7 cm/s. Optical windows were placed on the cell sides to allow real-time video monitoring and recording of the drilling process. The image was taken using a 210× magnification stereoscopic optical microscope, in combination with a CMEX 5 microscopy video camera, both placed above the cell, the optical axis of the microscope objective being perpendicular to the laser beam and water flow direction, and parallel to the irradiated surface of the target. The laser beam and water flow are perpendicular to each other. The image capture rate was 40 frames per second at a resolution of 640 by 480 pixels, and a pixel depth of 24 bits. An example of a frame is given in Fig. 2.

For each of the two target materials, the following laser pulse repetition rates were used: 500, 250, 100, 50 and 25 kHz. The energy per pulse corresponding to each repetition rate are 4.4, 7.4, 13.6, 20.6, 28.8 μJ, respectively. We chose the energy per pulse in order to maintain the drilling rate per second as constant possible for each pulse repetition rate.

In order to measure the hole depth as a function of irradiation time, drilling experiments were made for intermediary time intervals of 1, 2, 3, 4, 5, 10, 15, 20, 30, and 40 seconds for each case. The hole depths and diameters were measured with a UHL Rollscope TM2.

Both aluminum and steel targets were heat-treated at 300 °C in vacuum (~10^{-3} Pa) for one hour. This was necessary to prevent gas bubbles from developing on the target surface, obstructing the view and the laser beam. Even with heat treatment, in a few cases, when gas production was particularly abundant, artifacts due to the presence of gas bubbles appeared in the images.

3. Results and discussion

For each experiment, a total of 2000 frames were captured at 40 frames per second, corresponding to 50 seconds of laser irradiation of the target. For each of the frames, the sum of the pixel values was computed as a measure of light emission intensity. A graphic representation of the resulting numbers revealed a time evolution specific to laser pulse repetition rate and target material, as can be seen in Fig. 1. The scales and off-sets of the axes in Fig. 1 are adjusted so the temporal origin (starting moment of drilling) points and time interval coincide for the two data graphs, intensity emission and depth, respectively.

We found that emission intensity time evolution exhibits a specific pattern which changes according to material and laser repetition rate. Laser-matter interaction in a liquid environment presents a series of specific phenomena, the most notable being the confinement of the ablation plume. This results in development of a high temperature and high pressure plasma [9]. Many experiments [5, 6, 9-11, 13, 15] have indicated a massive increase in material removal rate and quantity due to plasma – target interaction and cavitation bubble collapse. In our case, the confinement is significantly stronger, since no free liquid surfaces are present.

Given the high repetition rate of the laser, the effects of successive laser pulses (debris, shock waves, cavitation bubble, collapsed cavitation bubbles, gas bubbles) can be expected to overlap, since such phenomena take place on a time scale of tens or even hundreds of microseconds [9]. It is therefore very likely that the noisy oscillation of the light emission intensity is caused by over-lapping effects in which the laser-target interaction is influenced by the effects of the previous pulses. At the moment, due to the low frame rate of the camera, it is difficult to draw a conclusion in regard to this possibility. A higher frame rate, followed by Fourier analysis might reveal some regularities in the form of consistent pulsating frequency spectra, which can be related to target material and laser repetition rate. Another possibility is that such an investigation will reveal chaotic behavior, since such phenomena can be expected to have such characteristics. Investigations in this directions will lead to important insights in laser-target interaction dynamics in a liquid environment. The effects produced by gas bubbles, which are particularly pronounced for the aluminum target at high laser repetition rates (500 and 250 kHz), are readily discernable as pronounced isolated peaks. This is possible, since the frames corresponding to the isolated peaks show abundant gas bubbles, as well as the presence of debris, as can be seen in Fig. 2.

After computing the emission intensity time evolution from recorded drilling processes, by comparing the graphs, it became apparent that the light emission intensity evolution follows the same pattern in all cases: a steep decrease in the first few seconds, followed by a less steep, or even constant evolution for the rest of the drilling process (Fig. 1). This pattern is particularly obvious in the case of aluminum drilling at 50 and 100 kHz (Fig. 1 b and c), and for steel drilling at 25, 50, 100 and 250 kHz pulse repetition rate (Fig. 1 f-i). It is worth mentioning that in the case of aluminum drilling at 500 and 250 kHz, the first stage is particularly short and steep, about 3 and 5 seconds respectively. In some cases, due to a more gradual transition between the two, there is an exponential-like evolution of the light emission (Fig. 1 b, c, h). The cause of this behavior is the variation in ablation plasma visibility. As the drilling advances, the plasma plume recedes into the target volume, becoming less visible. This corresponds to the first stage, with a steep decrease in emission intensity. After the view of the ablation plasma is completely obstructed, the camera receives light which originates from the laser beam and ablation plasma, and is then scattered off the debris/particulates/bubbles; this corresponds to a second, less steep evolution stage. The specific of each case is most probably due to a complex interplay between material removal mechanisms and laser shielding by plasma and particulates.

By correlating the graph with individual frames, we found that the pronounced isolated peaks, visible in figure 1d and e, can be attributed to light scattering on gas bubbles. As evidenced in Fig. 2, aluminum ablation in water at 500 kHz laser pulse repetition rate results in abundant gas production. This was in spite of the target being heat and vacuum treated, as mentioned in the experimental section. In fact, the purpose of the treatment was to prevent gas bubbles from sticking and forming on the target surface, not to prevent gas formation. Their effects consist in powerful laser scattering, causing the light emission intensity isolated spikes that can be seen in Fig. 1 e. A similar profile is present for 250 kHz, with a sudden disappearance for 100 kHz and lower laser repetition rates. This strongly suggests that the gas formation is related to local conditions, specifically to debris (particulate) concentration.
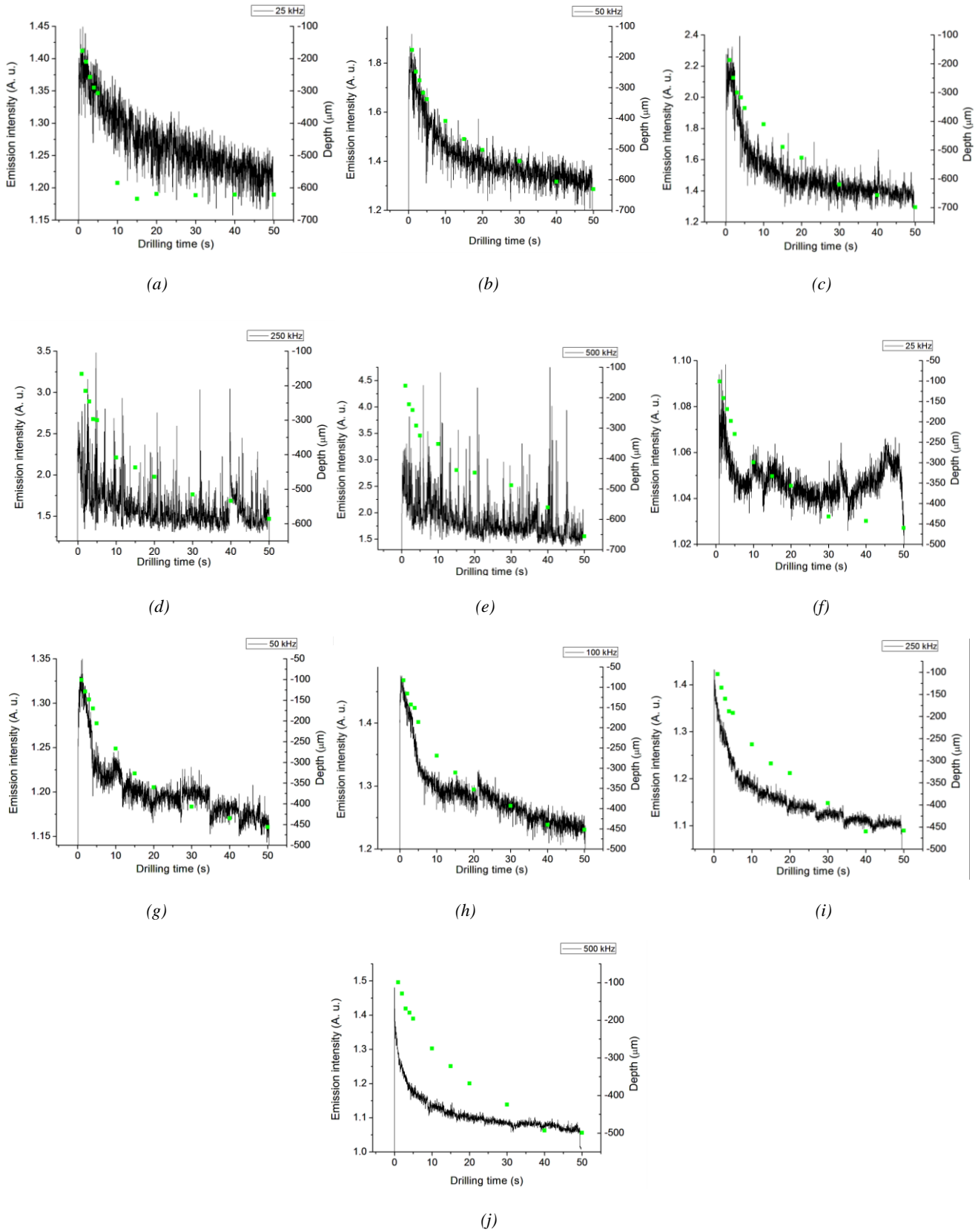
Fig. 1. Time evolution of emission intensity (black line, left y axis) and hole depth (green squares, right y axis). Aluminum a) to e) (left column). Industrial steel f) to j) (right column)

As evidenced in Fig. 1, by superposing graphs for light emission intensity and depth, in all cases at least a partial correlation between the two can be made. In the majority of cases (b, c, g-i) this correspondence can be for

the entire duration of drilling process. For a, d, e and f, this correlation can be made only for the first few seconds. The correspondence between the drilling depth and emission intensity is especially good (almost perfect overlapping) in the case of aluminum drilling with 100 and 50 kHz pulse repetition rates (Fig. 1 b and c). As mentioned in the introduction, we emphasize that it is not necessary for the graphs to superpose perfectly in order to correlate the depth with light intensity.
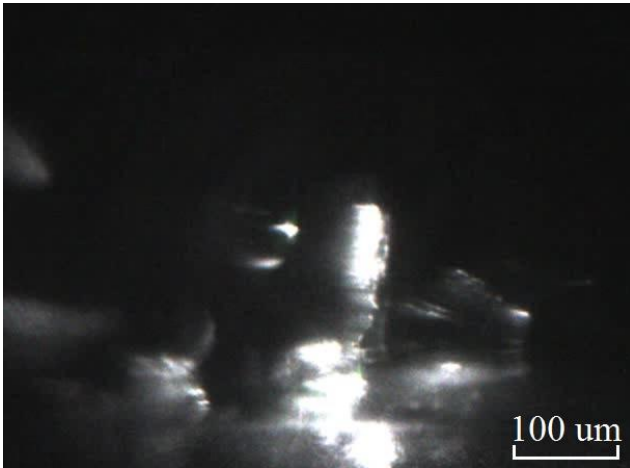

Fig. 2. Frame corresponding to one of the peaks in Fig. 1 e). Multiple light scattering zones (non-ablation plasma) are visible. All peaks correspond to similar frames, in which the light is scattered by high-density debris and/or gas bubbles

A puzzling case is presented in Fig. 1 d and e. It can be seen that the depth graph (green squares) mimics the light emission evolution to some degree, in the sense that two zones can be identified, a steeper zone followed by less steep one. In these particular cases, a correspondence between hole depth and light emission intensities can only be made for the first part of the graph. This is due to the fact that the second part of the graph is almost constant, in spite of the fact hole depth continues to grow. The interesting fact is that in the second zone, the depth continues to increase, but without a corresponding decrease in light emission. This might be due the abundance of particulate and gas bubbles, as evidence by the high spikes which are due to laser scattering on large gas bubbles.

Since the presence of bubbles may significantly hinder laser power delivery to the target [16], it is important to note the effects of target heat treatment in vacuum. In Fig. 3, the ablation of treated a) and b) non-treated steel targets are presented for comparison. On non-treated target, the view is completely obstructed by bubbles attached to target surface. At this stage, we can state that the heat treatment in vacuum eliminates a great quantity of air molecules adsorbed on targets surface. In case of non-treated target, the gas molecules presence on the surface facilitates bubble attachment, and it might also lead to bubble nucleation and growth.
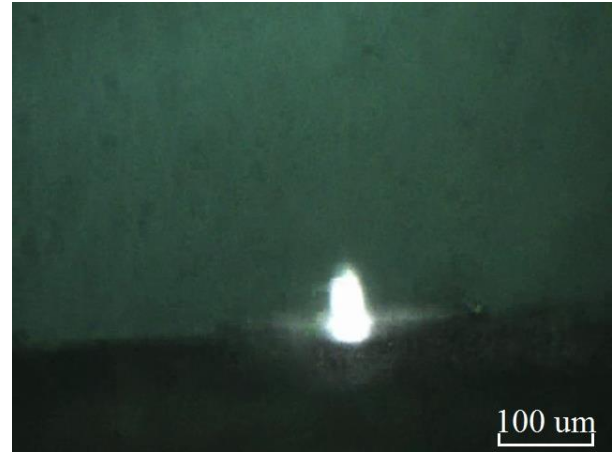

(a)
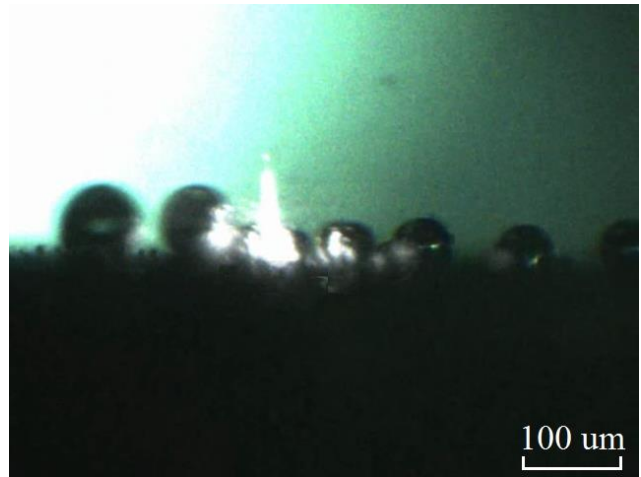
(b)

Fig. 3. Heat and vacuum treated steel target a), vs. untreated b). In image b) gas bubbles attached to the target are visible

In general, visible light emissions in laser-matter interactions are due to excited species in the plasma plume, as well as light from both laser and ablation plasma scattering on ablation products. At any given moment, the camera registers the combined effect of all emission mechanisms, and any intensity variation is caused by variations of one or more of them. In the following, we will refer occasionally to the light emitting volume, which accounts for all phenomena, light scattering volume and ablation plasma plume. It is expected that a light scattering zone will envelop the ablation plume. In some cases, there is a clear distinction between ablation plasma and debris, as can be seen in Fig. 2.
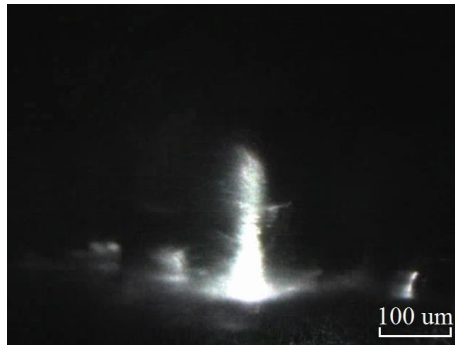
(a)

(b)

(c)

(d)

Fig. 4. Aluminum ablation at a) 500, b) 100, c) 50 and d)
25 kHz repetition rates

In Fig. 4, large ablation plumes with a debris zone extended perpendicular to the target direction are visible. The general aspect is rough and uneven due to particulates and gas bubbles. Fig. 4 a) presents an image of a turbulent ablation process in the case of aluminum laser ablation at 500 kHz laser repetition rate. A high density of debris and gas bubbles is visible. Nevertheless, the image presented here is a "regular" one, in contrast with that shown in Fig. 2. The image obtained for 250 kHz (not given here) is similar, as the similar light intensity emission graphics indicate. As the laser repetition rate is reduced to 100 kHz (Fig. 4 b), a sharp decrease in turbulent scattering zones, present in 4 a) is visible. An extended scattering zone due to the abundance of debris, which is a result of high material removal facilitated by the low ablation threshold and mechanical resistance of aluminum. The right side of the light emitting volume is sharper then the left side, corresponding to the direction of water flow (from right to left).

In the case of steel presented in Fig. 5, a smaller and more homogenous light emitting zone, with no rough areas, is present. It can be seen that even at 500 kHz, the drilling process is steady, due to the lower material removal rate than in the case of aluminum. In Fig. 5 a), the debris light-scattering zone is visible as a glow around the plasma plume. At 100 kHz laser repetition rate (Fig. 5 b), a slightly smaller and less bright light emitting volume is visible. An asymmetry of the light emitting zone, caused by water flow, can be observed. This and 50 kHz are the only cases in which this asymmetric aspect is present.

As the repetition rate further decreases to 50 kHz, a smaller and dimmer light emitting volume is present in fig. 5c, but still retains the same general aspect. The sharpness on the right side becomes even more evident. At this point, it seems that a significant part of the light emitting volume consist in light scattering debris. At 25 kHz repetition rate, the aspect of the light emitting volume is dramatically changed (Fig. 5 d). Judging by its appearance, it probably consists in debris-scattered light only.

The main cause for the intensity variation is due to the increase of drilling depth, as the laser-target impact zone recedes inside the target volume, with the resulting fluence reduction. As debris are ejected outwards, a laser scattering zone is expected to persist at the target surface as long as material is still being removed from the target, even if no ablation plume is visible. A reduction in light intensity will also occur, since as the amount of ablated material decreases due to laser fluence reduction, so does the light originating from ablation plasma.

(a)

(b)

(c)

(d)

Fig. 5. Images of steel ablation for a) 500, b) 100, c) 50 and d) 25 kHz

Table 1. Light emission intensity (in arbitrary units a.u.) for each material and laser repetition rate, at the beginning of the drilling process

Target material	Laser repetition rate (kHz)				
	500	250	100	50	25
	Light emission intensity (a. u.)				
Aluminum	2.9	2.29	2.24	1.82	1.4
Steel	1.48	1.43	1.47	1.33	1.07

In Table 1 the maximum values for light emission intensity are given. The maximum value of the light emission intensity was taken, excluding the isolated peaks originating from light scattering on gas bubbles. The steady decrease in the case of aluminum is due to the scattering origin of light. As the repetition rate decrease, so is the density of debris encountered by the laser beam, as the water flow clears them out of the path of the laser beam. In case of steel this value is much lower, almost half the maximum for aluminum. This is due to the higher ablation threshold of steel, which results in a smaller plasma plume, and lower debris and gas bubble generation rate. The very slow decrease the case of steel might also be due to the fact that the light originates mainly from excited ablation plasma species.

Regarding bubble formation, it is relevant that in the case of aluminum, as the repetition rate decreases, so does gas formation. This signifies that much of the gas formation is debris-mediated and laser-induced. As the repetition rate decreases, so does the density of the debris encountered by laser radiation, which lead to less gas formation.

4. Conclusions

The light emission from both excited species in the ablation plasma and laser scattering were studied by recording images with a 210× optical stereoscopic microscope. By image digital processing, a measure of the light emission was obtained as a summation of all pixels composing each frame of the recording.

All of the light emission intensity behaved in the same two stage pattern: a sharp decrease followed by a slow decrease or, in some cases, a constant value. The key finding of these experiments consists in the possibility of in-situ monitoring of the drilling depth.

In the case of aluminum, one may conclude that significant light emission originates from light scattering, since a systematic and pronounced decrease in intensity is observed following the decrease in laser repetition rate. Steel ablation, on the other hand, has a much lower particulate and gas production rate than aluminum. In addition, a significantly lower light level and variations suggest a lower particulate dimension for steel.

While not suitable for probing drilling dynamics with a high temporal resolution due to reduced frame rate, this method is capable of offering indications about the tendency of the drilling process. Its main advantage consists in its capability to record indefinite lengths of

time, while a high speed camera would be limited to only a few seconds.

This type of recording allows precise measurements of plasma dimensions, and, consequently, its evolution during the drilling process can be evaluated. Precise dynamics of the debris can be seen in the images, along with the water flow. Automated image processing could be performed in order to evaluate the quantity of debris, their relative energy, dimensions, etc. All this information can be extracted from the video recording of the drilling process, but requires developing special software tools. Given the complexity of the phenomenon captured in the recordings, processing automation to extract detailed information will be a challenging, but not unfeasible, task.

In this work, we were interested in the light emission originating in the drilling process itself only, and, consequently, we have not used a secondary light source. By using one, it is expected that new types of information could be extracted, as it would enable debris tracking on a larger length scale.

Acknowledgements

References

[1] K. Wu, Z. Xia, F. Kong, Y. Jin, J. Optoelectron. Adv. M. **20**(5-6), 258 (2018).

[2] M. S. Iovu, S. A. Sergeev, O. V. Iaseniuc Optoelectron. Adv. Mat. **12**(7-8), 377 (2018).

[3] C. Sima, W. Waldhauser, J. Lackner, M. Kahn, I. Nicolae, C. Viespe, C. Grigoriu, A. Manea, J. Optoelectron. Adv. M. **9**(5), 1446 (2007).

[4] E. Chan y Diaz, M. Acosta, R. Castro-Rodriguez, A. Iribarren, J. Optoelectron. Adv. M. **19**(7-8), 506 (2017).

[5] M. E. Shaheen, J. E. Gagnon, B. J. Fryer, Journal of Applied Physics **113**, 213106 (2013).

[6] P. Ouyanga, P. Lia, E. G. Leksinac, S. V. Michurinc, L. Heda, Applied Surface Science **360**, 880 (2016).

[7] S. Barcikowski, A. Menéndez-Manjón, B. Chichkov, M. Brikas, G. Račiukaitis, Appl. Phys. Lett. **91**, 083113 (2007).

[8] N. Baersch, A. Gatti, S. Barcikowski, JLMN-Journal of Laser Micro/Nanoengineering **4**, 66 (2009).

[9] Dynamics of Liquid-Phase Laser Ablation, K. Sasaki in Laser ablation in liquids – principles and applications in the preparation of nanomaterials, edited by Guowey Yang, Pan Stanford Publishing Pte. Ltd., Singapore, (2012).

[10] T. Sakka, K. Saito, Y. H. Ogata, Journal of Appl. Phys. **97**, 014902 (2005).

[11] N. Takada, T. Nakano, K. Sasaki, Appl. Phys. A **101**, 255 (2010).

[12] S. Himeno, T. Kato, K. Urabe, S. Stauss, S. Kato, H. Muneoka, M. Baba, T. Suemoto, K. Terashima, IEEE Transactions on Plasma Science **42**, 2630 (2014).

[13] N. Takada, T. Nakano, K. Sasaki, Applied Surface Science **255,** 9572 (2009).

[14] T. T. Phuong Nguyen, R. Tanabe, Y. Ito, Applied Physics Express **6**, 12270 (2013).

[15] I. Nicolae, M. Bojan, C. Viespe, D. Miu, Micromachines **8**, 316 (2017).

[16] C.-H. Tsai, C.-C. Li, Journal of Materials Processing Technology **209**, 2838 (2009).

_____

[*]Corresponding author: cristian.viespe@inflpr.ro